2021 43rd Annual International Conference of the
IEEE Engineering in Medicine & Biology Society (EMBC)
Oct 31 - Nov 4, 2021. Virtual Conference

A Combined Deep Learning and Anatomical Inch Measurement Approach to Robotic Acupuncture Points Positioning

Tai Wing Chan, Chris Zhang, Wai Hung IP, Alex WH Choy

Abstract: **Acupuncture therapy is one of the cornerstones in traditional Chinese medicine. It requires rich experiences from Chinese medicine practitioner. However, repeatability among different practitioners are low. Meanwhile, there is a large variety of skin conditions in terms of color, diseases, size, etc. In recent year, deep neural network for acupuncture point detection is proposed. However, it is difficult to localize multiple acupuncture points. In this paper, a high repeatability robot with a new approach of acupuncture points positioning is proposed which can be adaptive to variety skin conditions and achieve multiple acupuncture points' localization.**

Clinical Relevance— **This system can provide identical acupuncture therapy to different patients. Thus, the quality of the therapy can be practitioner independent. Furthermore, the machine operation is simple therefore manual error can be reduced significantly. As the result, the efficiency and accuracy of therapy can be increased.**

I. INTRODUCTION

Traditional Chinese Medicine and Western Medicine are two major different disciplines of healing. In traditional Chinese medicine, acupuncture therapy is a historical approach and widely applied in many countries. In order to train a Chinese medicine practitioner to be a professional acupuncturist, it requires time and practical experiences. More than 2000 training hours are required in order to complete the entire acupuncture practitioners training [1]. Therefore, the number of professional acupuncture practitioners is hard to fulfill the demand from patients. Furthermore, it is difficult to promise the qualities of acupuncture therapy between different professionals are identical since manual operation is difficult to ensure the repeatability. As the result, an automated approach can help to tackle the current situation. The approach can help professional Chinese medicine practitioner to perform acupuncture therapy after they choose the correct points and orders. The machine can recognize multiple points and perform therapy with high repeatability robotic arm. As the result, professional practitioners' workload can be reduced and beginners of Chinese medicine practitioners are able to learn from the automated system.

Different acupuncture points' detection approaches were proposed. Park et al. [2] proposed to detect those acupuncture points with electrical properties. They transformed human skin properties to an equivalent electrical circuits .They developed a microcontroller system to read and demodulate electrical impedance data from variable frequencies. Chang and Zhu [3] investigated an automatic facial acupuncture points positioning system with facial features analysis using image processing techniques. Canny edge detector algorithm and face recognition algorithm are used to perform feature extractions. In the latest research, Sun [4] investigated an approach to detect two acupuncture points with a deep convolutional neural network, one kind of deep learning methods [5]. A customized dataset was used to train the deep convolutional neural network thus it was able to recognize the two acupuncture points near the joints.

Acupuncture points positioning is the first step of acupuncture therapy. A high precision machine is required to perform precise therapy operations. Su [6] investigated to control the robotic arm with vision and force sensing precisely. It was able to respond to when the needle hits the bone. Lan and Litscher [7] showed that Hand-Eye Calibration was able to assist acupuncture therapy. Their system connected the coordinate relationships between camera and robotic arm. By calculating the transformation, the acupuncture points detected in the camera was projected to the workspace of the robotic arm. Xia et al. [8] developed a redundancy strategy to ensure the safety of the robot. A task and data synchronization method is proposed based on the crystal oscillator with a master-slave hardware architecture. The system was simulated in OMNeT++ and the result was satisfactory.

In the current stage, supervised deep learning starts to be a solution of acupuncture point detection due to its adaptability and flexibility. It is able to foresee more artificial intelligence based application will be introduced in medical system. However, samples among different patients have a large diversity. There may be skin diseases and even tattoos which may potentially affect some feature based deep learning system. Furthermore, it is hard and time consuming to collect and label a dataset for each individual acupuncture point. Therefore, we proposed an approach to detect acupuncture points with the deep convolutional network. We integrated the body parts detection which is performed by deep learning and locate the acupuncture points by Chinese anatomical measurement (cun). Thus, a general human body dataset can be shared to reduce the preparation time of dataset preparation and the acupuncture points were located based on cun measurement and calculations in the area specified by deep learning. In this approach, the skin diseases or other skin features did not affect the positioning system. With the help of cun measurement, multiple points of acupuncture points were recognized simultaneously. Potentially, it is able to perform acupuncture positioning on different human parts. After the acupuncture point positioning system was executed, the coordinates of acupuncture points in the image were transformed to the robotic arm control system to perform therapy.

The organization of this paper was as follows. Section II is about the details of proposed system and workflow which contains the integration of human part detection and cun measurement. Meanwhile, the transformation between image coordinates and robotic arm workspace is discussed. Next, experimental results analysis is evaluated in Section III. The last section is about conclusions and future works.

II. PROPOSED SYSTEM AND WORKFLOW

This section is about the proposed system and workflow of the automated acupuncture system including the deep learning human part detector, mesh of cun measurement, coordinates transformation and robot control. The general system architecture was displayed in Fig 1. Patient was required to place his/her upper limb stationary under a clean background and allowed the robot to capture the image. When the captured image was ready, deep convolutional neural network started to analyze and detect the human part in it. A mesh was then generated based on the output boundary box using cun measurement. When the mesh was generated, several acupuncture points were located thus they were transformed to the robot and perform acupuncture therapy.

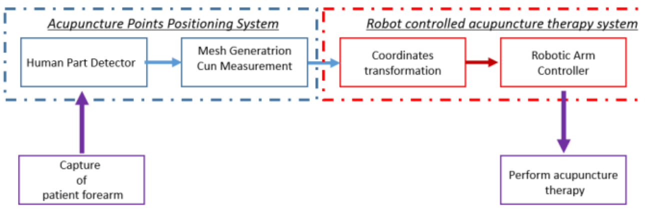

Figure 1. System architecture

A. Human Part Detector

The deep convolutional neural network used in this system was SSD-MobileNet v1 and deployed in NVIDIA Jetson TX2. As Howard et al. [9] investigated that the depthwise separable convolution was the combination of depthwise convolution and 1x1 pointwise convolution. This approach helped to accelerate the inference time of the network with satisfactory accuracy by reducing the complexity of computing. Lui et al. [10] proposed that Single Shot Detector (SSD) was able to produce detections by adding the auxiliary structure to a base network. Therefore, in SSD-MobileNet v1, Mobilenet is the base network for feature extraction. Meanwhile, SSD was used to perform classification and boundary box regression [11]. The network feature pyramid of the model was shown in Fig 2.

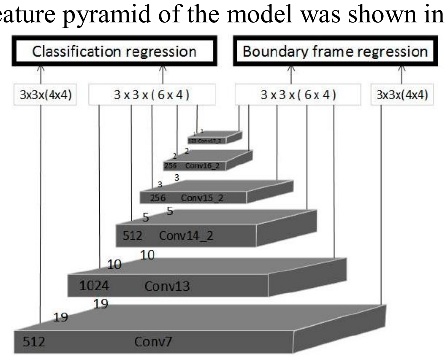

Figure 2. SSD Mobilenet feature pyramid [11]

The deep convolutional neural network was trained to recognize the human parts and locate it using a boundary box. The loss function was expressed in the following [10].

$$L(x,c,l,g)=\frac{1}{N}(L_{conf}(x,c)+\alpha L_{loc}(x,l,g)) \quad (1)$$

L_{loc} was assumed to be the localization loss between the predicted boundary box and the ground truth box. L_{conf} was assumed to be the loss between SoftMax multiple classes classification and the ground truth class. N was the number of matched boundary boxes.

B. Mesh generation with Chinese anatomical Measurement

Chinese anatomical measurement is the approach for Chinese medicine practitioner to search and locate the acupuncture points. A measurement or scale is defined independently based on different parts of human body. With the help of human part detector, different meshes with corresponding scales were generated for different human parts. Those meshes were useful to calculate the positions of acupuncture points.

The output of a human part detector was a boundary box with four coordinates named as A (x_i,y_i), B (x_i,y_j), C (x_j,y_i) and D (x_j,y_j) *where* $x_j>x_i$ and $y_j>y_i$. These four points located the workspace of a mesh. In order to locate the mesh precisely, these four coordinates were shrunk to the surface of a human part. Thus, a polygon is formed. The shrinking process was determined by a threshold after RGB To HSV conversion with simple and uniform background which can be expressed as the following [12].

$$H = \arccos\frac{\frac{1}{2}(2R - G - B)}{\sqrt{(R - G)^2 - (R - B)(G - B)}} \quad (2)$$

$$S = \frac{\max(R , G, B) - \min(R ,G , B)}{\max(R, G, B)} \quad (3)$$

$$V = \max(R, G, B) \quad (4)$$

Thus, four anchors were the resultant output determined by HSV thresholding which were named as $\alpha\,(x_i,y_i+\Delta y)$, $\beta(x_i,y_j-\Delta y)$, $\gamma\,(x_j,y_i+\Delta y)$ and $\delta(x_j,y_j-\Delta y)$ in Fig 3. Δy was considered as the movement of those four anchors.

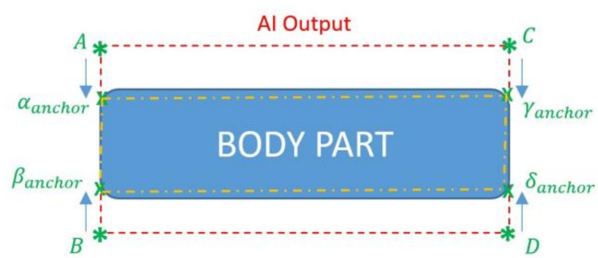

Figure 3. Basic mesh generation

With the basic mesh generated, the Chinese anatomical measurement was able to be deployed. Coyle et al. [13] claimed that acupuncture points were distributed along different Meridians with different cun units. Assume that body part contained N cun and M meridians, N unit of cun and M meridians were defined in this mesh and expressed in the following equations and Fig 4.

$$x_{cun\_n}= x_i+ndx \text{ where } n=0,1,\ldots,N \quad (5)$$

$$f_{meridan\_m}(x)=\left(\frac{b_{m2}-b_{m1}}{a_{m2}-a_{m1}}\right)x+c \text{ where } m=1, 2,\ldots,M \quad (6)$$

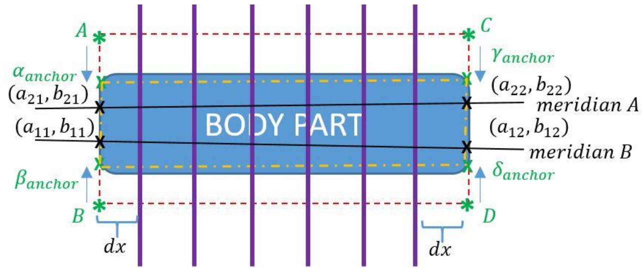

Figure 4. Mesh generated with Chinese anatomical measurement

With the resultant mesh, multiple acupuncture points on the specific body part were possible to be searched. By combining the medical definition of an acupuncture point, it helped to define the starting and ending position (a and b) in (6) of a meridian and the number of cun units (n) in (5). By resolving the x_{cun_n} and $f_{meridan\_m}$, a specific acupuncture point position was located. As the result, different acupuncture points were able to be located with this approach. Furthermore, it was not affected by any features within the body part such as skin diseases.

C. Coordinates transformation for robotic arm

Different acupuncture points were localized with the above approach within a specific body part. Those points supposed to be the goal of the end effector of a robotic arm. Thus, a transformation between image space and robotic arm workspace was required. Ito [14] reported that the transformation between the image space coordinates and world coordinates was achieved by a rotational matrix and lens perspective projection principle in Fig 5.

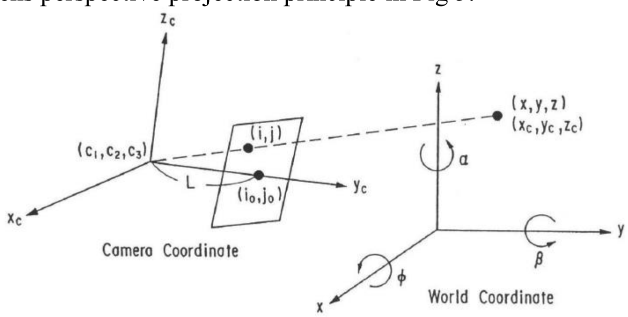

Figure 5. Coordinates transformation from camera to world [14]

III. EXPERIMENTS AND EVALUATIONS

In the following experiments, no human subjects nor animals were involved. In order to evaluate the system, forearm was taken as a body part to perform acupuncture points detection. Therefore, a human forearm dataset was prepared for deep convolutional neural network training. It was a small dataset which contained 278 images. 30% of the images were used for testing. The training was executed in Nvidia DGX2 system with Tensorflow framework. Furthermore, 5 acupuncture points on the forearm were chosen which were labelled from 0 to 4 in Table I [15]. By deploying the trained neural network, the mesh generation was evaluated. The mesh helped to locate those acupuncture points and prepared to be transformed to the robot workspace.

TABLE I. ACUPUNCTURE POINTS DEFINITION[15]

Index	**Acupuncture Points**		
	Name	***Cun Unit***	***Meridian***
0	PC 7-Great Mound	0	The Pericardium Meridian
1	HT 7-Spirit Gate	0	The Heart Intestine Meridian
2	LU 9-Very Great Abyss	0	The Lung Meridian
3	LU 5-Outside Marsh	12	The Lung Meridian
4	HT 3-Lesser Sea	12	The Heart Meridian

Furthermore, Coyle et al. [13] reported that the total distance between the elbow crease and the wrist crease was 12 cun. Therefore, N should be 12 in (5). Lightbody [15] reported that there are three types of meridian in the area of human forearm thus M equals to 3 in (6). The detailed positions of different acupuncture points were shown in Fig 6.

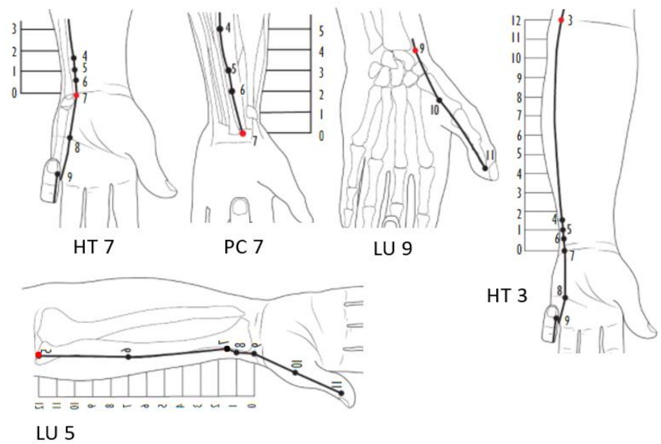

Figure 6. Locations of chosen acupuncture points [13]

A. Human Part Detector (Forearm)

There were total 200000 epochs in training. The loss started to converge and stabilize at the 50070th epoch. Therefore, the output of the network will be deployed by the training result at 50070th epoch in Fig 7. The total loss was 0.6149. Meanwhile, the localization and classification loss were 0.01014 and 0.2705. During experiment, forearms with different skin conditions were used to test the detector. There were patients with atopic dermatitis, different skin colors and different hair density. The results showed that the detector was independent of skin conditions or skin diseases in Fig 8. Therefore, it can help to locate the mesh under various conditions since the skin conditions of different patients were not consistent.

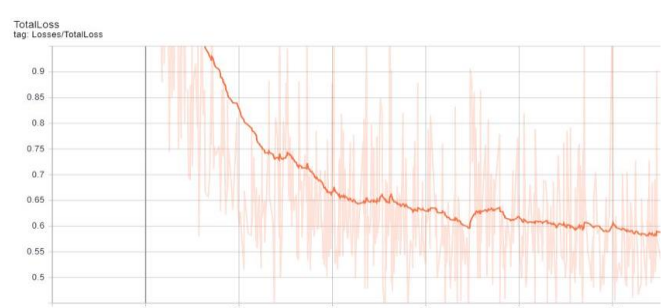

Figure 7. Total loss of the training (smoothed with 0.975)

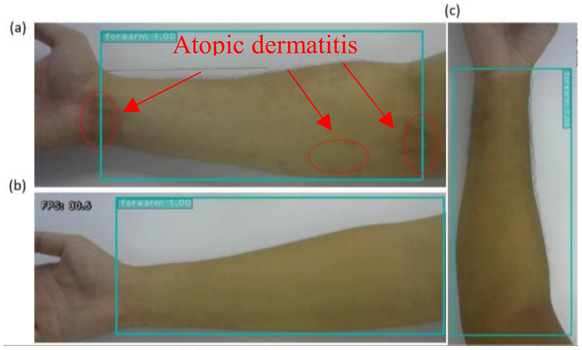

Figure 8. (a) an adult male forearm with atopic dermatitis, (b) a healthy adult female forearm, (c) a hairy adult male forearm

B. Mesh generation and acupuncture points positioning

The success of forearm detector helped to generate the mesh. As Sun [4] proposed an approach to evaluate the offset error, the same approach was deployed in (7). The offset error of an individual acupuncture in an image was defined by a normalized Euclidean distance where P_i and P'_i were the coordinates of predicated and ground truth acupuncture points. Noted that d was the distance of the forearm in an image.

$$\text{offset error} = \frac{\|P_i - P'_i\|_2}{d} \tag{7}$$

The result was satisfactory, see Table II. Sun [4] reported that a threshold of 0.08 helped to define the success of the positioning system by taking average length of an adult forearm and the average radius of a finger's contact surface area. Most of the points full filled the requirement. The sample output of the mesh generation was show in Fig 9.

TABLE II. OFFSET ERROR EVALUATIONS

Acupuncture Points	Average offset error	Number of samples
PC7	0.0428561 < 0.08	50
HT7	0.050624832 < 0.08	50
LU9	0.051542877 < 0.08	50
LU5	0.054821251 < 0.08	50
HT3	0.092837094 > 0.08	50

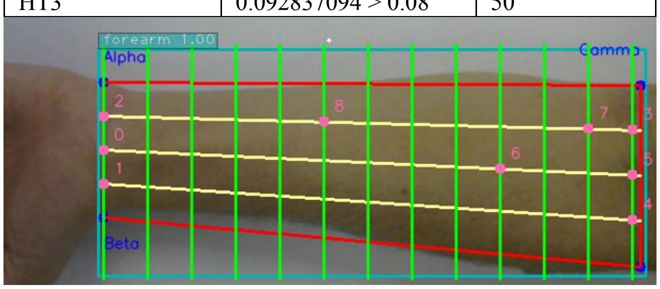

Figure 9. Resultant mesh generation

C. Robotic Arm acupuncture simulation

Different acupuncture points were located. However, the linkage between the image space and robot workspace had to be established. With the help of robot operating system (ROS), it transformed and visualize the acupuncture points under robot workspace in Figure 10. Those vectors represented the acupuncture points and the blue cuboid defined the boundary box from the deep learning detector.

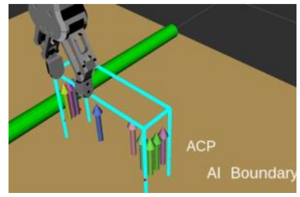

Figure 10. Visualization of acupuncture points in robot workspace

IV. CONCLUSION

The system was able to identify multiple acupuncture points under various skin conditions with satisfactory performance. More points were detected in different human body part if a richer database and anatomical distributions are collected. One limitation of the proposed system is that the orientation of insertion is not considered, which will be our future work. Another future work is regarding the optimal design of such robots, by for example force balancing [16] that can perform the task precisely.

REFERENCES

[1] *Guidelines on basic training and safety in acupuncture*. Geneva: World Health Organization, 1999.

[2] H. D. Park et al., "A New Acupuncture Point Detection Using the Impedance Measurement System Based on ANF and Phase-Space-Method", *2007 29th Annual International Conference of the IEEE Engineering in Medicine and Biology Society*, pp.2572-2574, 2007.

[3] M. Chang, Q. Zhu, "Automatic location of facial acupuncture-point based on facial feature points positioning", *2017 5th International Conference on Frontiers of Manufacturing Science and Measuring Technology (FMSMT 2017)*, pp.545-549, 2017.

[4] L. Sun, S. Sun, Y. Fu and X. Zhao, "Acupoint Detection Based on Deep Convolutional Neural Network", *2020 39th Chinese Control Conference (CCC)*, pp.7418-7422, 2020.

[5] W.J. Zhang et al., "On Definition of Deep Learning", *2018 World Automation Congress (WAV)*, pp. 1-5, 2018.

[6] J. Su, Y. Zhu and M. Zhu, "Hand-Eye-Force Coordination of Acupuncture Robot", *IEEE Access*, vol. 7, p.82154-82161, 2019.

[7] K.C. Lan, G. Litscher, "Robot-Controlled Acupuncture-An Innovative Step towards Modernization of the Ancient Traditional Medical Treatment Method", *Medicines(Basel, Switzerland)*, vol. 6, no. 3, pp.87,2019.

[8] X. Xia, H. Sun, D. Wu and Z. Wang, "Research on Controller Redundancy Strategy of Acupuncture Robot", *2019 International Conference on Electronic Engineering and Informatics (EEI)*, pp.341-345, 2019.

[9] A. G. Howard et al., "MobileNets: Efficient Convolutional Neural Networks for Mobile Vision Applications", *arXiv:1704.04861*, 2017.

[10] W. Lui et al., "SSD: Single Shot MultiBox Detector", *European conference on computer vision*, pp.21-37, 2016.

[11] Y. Li et al., "Research on a Surface Defect Detection Algorithm Based on MobileNet-SSD", *Applied Sciences*, vol. 8, no. 9, pp.1678, 2018.

[12] K. B. Shaik et al., "Comparative Study of Skin Color Detection and Segmentation in HSV and YCbCr Color Space", *Procedia Computer Science*, vol. 57, no. 12, pp. 41-48, 2015.

[13] M. Coyle et al., "The Cun Measurement System: an Investigation into its Suitability in Current Practice", *Acupuncture in Medicine*, vol. 18, no. 1, pp. 10-14, 2000.

[14] M. Ito, "Robot vision modelling-camera modelling and camera calibration", *Advanced Robotics*, vol. 5, no. 3, p. 321-335, 1990.

[15] S. Lightbody, *The 361 classical acupuncture points: names, functions, descriptions and locations*. Singapore: World Scientific, 2020.

[16] P. Ouyang and W.J. Zhang, "Force Balancing of Robotic Mechanisms Based on Adjustment of Kinematic Parameters", *ASME Journal of Mechanical Design*, vol. 127, no. 3, pp. 433-440, 2005.